



CLIC Post-collision Diagnostics

V. Ziemann, Uppsala University

April 13, 2008

Abstract

We discuss non-conventional diagnostics for the beam line between the interaction point and the beam dump of CLIC. The main focus is put on the beamstrahlung monitor, but also other systems such as a coherent pair monitor, tail monitors, and interferometric beam dump thermometer are considered.

1 Introduction

The Compact Linear Collider (CLIC) with a center of mass energy of 3 TeV is envisioned to do precision spectroscopy of new particles found at LHC. In order to achieve reasonable count rates very high luminosities in the $10^{34}/\text{cm}^2\text{s}$ range are needed which entails that extremely small beam sizes at the interaction point (IP) are required which are on the order of $100\text{ nm} \times 1\text{ nm}$. After the collision the beams have to be transported to their respective beam dumps which can be problematic in both cases of actually colliding or missing each other. If the beams collide, they are violently disrupted in the electromagnetic field of the counter-propagating target beam and the increased momentum spread and angular divergence make it difficult to reach the dump without losses on the way. If the beams are missing each other, the bunches maintain their small size on the way to the dump and will result in extreme densities on the small point of impact on the dump window.

The first problem with losses in the beam line was addressed in Ref. [1] and resulted in a beam line with a minimal number of components. Only a vertical chicane is foreseen to separate the beamstrahlung and opposite-charge coherent pair partners from the primary beam. The aperture of the dipole magnets and the vacuum beam pipe are large to minimize particles losses. The second problem with the heat load on the window was addressed in Ref. [2] and resulted in a thin vacuum window tailored after the LHC dump window. Since parameters in either case are rather tight it will be necessary to monitor the beam parameters and determine whether the beams are in collision to guarantee machine protection and during startup it will be essential to have diagnostic equipment to find out whether the beams are in collision or at least close to collision. Once collisions are established, monitoring the luminosity on fast time scales will be essential for routine operation of CLIC [3].

In this report we therefore investigate the potential to integrate diagnostic for luminosity in the post-collision beam line between the IP and the dump. We stress that this is an extremely hostile environment due to high radiation levels that will destroy anything exposed directly to the beam which implies that non-invasive diagnostic devices are needed. In the following sections we discuss a compilation of devices that could prove useful in extracting important information from the beam, partly by analyzing the temperature distribution in the beam dump, image charges in the beam pipe, or various types of radiation emanating from the IP.

We stress that we focus on the instrumental side of the monitors in this report. Establishing the correspondence of the detected signals to the luminosity is relegated to a separate note. We mostly focus on the beamstrahlung detector, but also investigate the suitability of other detectors for the post-collision line in later sections of this report.

2 Beamstrahlung

In order to be able to maintain the beams in collision a fast signal, that is related to the luminosity is needed [3], preferably with a temporal resolution short compared to the

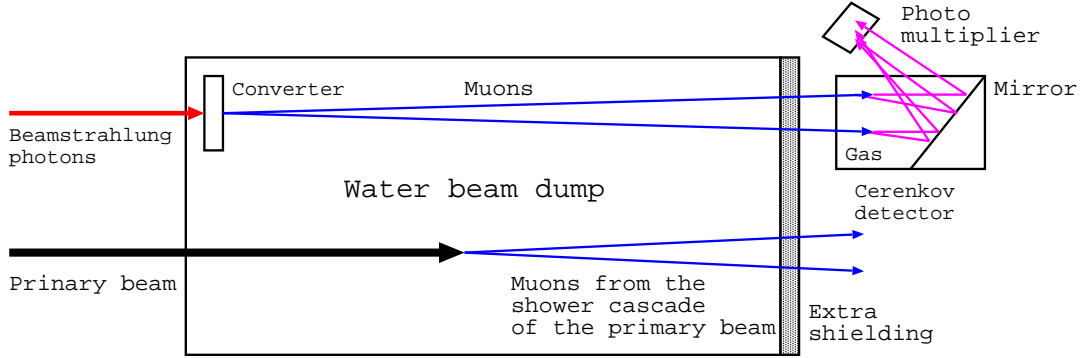


Figure 1: Cerenkov beamstrahlung detector based on the conversion of high-energy beamstrahlung photons into muon pairs, that are the only charged particles penetrating the beam dump and can be detected by their emission of Cerenkov light in a gas detector. Note that the high-energy muons generated from the primary beam are predominantly forward peaked and miss the Cerenkov detector.

duration of the bunch train. An adapted version of the SLC beamstrahlung detector [4], might provide this. The notable difference of the original monitor to the CLIC monitor is that we suggest to use muons to generate the Cerenkov light due to the much higher beam energy in CLIC. The layout of the detector is shown in Fig. 1, where the beamstrahlung photons impinge on the beam dump from the left and pass the entrance window and possibly a converter plate that converts the photons predominantly to electron and muon pairs. Since the converter plate is embedded in the water dump, we assume that it will sustain the energy deposited. Optimization to balance the number of muons created and the heat load will need to be done. All products of the shower that ensues, except most of the muons, will be absorbed in the remainder of the beam dump and additional shielding. Only the muons will be able to penetrate the dump enclosure. We suggest to place a gas volume behind the beam dump in which the muons will generate Cerenkov radiation that can be picked up by a photo multiplier tube.

Not only the beamstrahlung photons from the beam-beam interaction will reach the upper section of the beam dump foreseen for beamstrahlung, but also a large amount of synchrotron radiation from the dipole magnets of the chicane that bend the primary beam downwards. The maximum beam energy foreseen in CLIC is $E = 1.5$ TeV and for the dipole field we assume $B = 1$ T which results in a critical energy ε_c of the synchrotron radiation photons of

$$\varepsilon_c[\text{keV}] = 0.665E^2[\text{GeV}]B[\text{T}] = 1.5 \times 10^6 [\text{keV}] \quad (1)$$

or $\varepsilon_c = 1.5$ GeV. We therefore need a detector with a threshold that discriminates photons with energies below a few GeV.

The advantage of the Cerenkov detector setup is that it provides a threshold and it also relies on the detection of particles that can penetrate heavy shielding. This is similar to

the way that large particle detectors such as ATLAS at LHC have muon chambers all around the outer layer beyond the iron yoke. Thus this detector discriminates unwanted contamination from low-energy particles. The second level of discrimination comes from the Cerenkov detector which only detects particles above a threshold, given by

$$\beta_0 n > 1 \quad \text{or} \quad \gamma_0 > \frac{n}{\sqrt{n^2 - 1}} \quad (2)$$

where $\gamma_0 = 1/\sqrt{1 - \beta_0^2}$ is the energy of the muon in units of its rest mass and β_0 is its speed in units of the speed of light c . The symbol n denotes the refractive index of the rarefied gas. Other means of detection different of Cerenkov light are also possible, but photo-multiplier give a very fast signal that is related to the muon flux, which in turn depends on the beamstrahlung photon flux that is related to the luminosity. We need to stress that the primary beam will also generate muons that will be separated vertically from the muons from beamstrahlung. Due to the high beam and photon energy most of the muons will be strongly forward peaked and only a small fraction might scatter into the detector. This will need to be investigated in a more comprehensive later study. Another potential problem can arise from the fact that the beam dump is rather close to the beam line of the counter-propagating primary beam line which could perturb the detector. We do not anticipate a big problem, because the mirror in the gas volume is direction sensitive and only images light going from left to right in Fig. 1 into the photo-multiplier.

We now follow Refs. [5, 6, 7] to estimate the number of Cerenkov photons as a function of the incident beamstrahlung photon energy and later convolute this with the beamstrahlung spectrum. We observe that the pair production in the converter plate is approximately given by the Bethe-Heitler cross-section for ultra-relativistic particles [8] with the electron mass replaced by the muon mass m_μ

$$\sigma = \frac{28}{9} Z^2 \alpha r_\mu^2 \left(\ln \frac{2\hbar\omega}{m_\mu c^2} - \frac{109}{42} \right) \quad (3)$$

where r_μ is the classical muon radius, $\alpha = 1/137$ is the fine-structure constant, and Z is the atomic number of the converter material. For iron with $Z = 26$ and $\hbar\omega = 100 \text{ GeV}$ photons we find $\sigma = 141 \mu\text{barn}$. The probability to convert the incident photon with energy $\hbar\omega$ into a muon pair is then given by

$$P = 1 - e^{-nd\sigma} \approx nd\sigma \quad (4)$$

where $n = 8.4 \times 10^{22}/\text{cm}^3$ is the number density of iron and d is the thickness of the converter. With a thickness $d = 1 \text{ mm}$ we find a conversion rate of $P = 1.2 \times 10^{-6}$, only about one in a million photons results in a muon pair. It is useful to compare this to the muon production in the 15 mm carbon window discussed as the entry window to the beam dump [2]. The cross section σ is reduced by $(6/26)^2$ to $7.5 \mu\text{barn}$, the thickness is increased by a factor of 15 mm/1 mm and the number density $n = 7.5 \times 10^{22}/\text{cm}^3$ is roughly equal to that of iron. The corresponding probability P_C for the carbon window is thus $P_C = 0.8 \times 10^{-6}$ or about 30% less than the 1 mm iron converter.

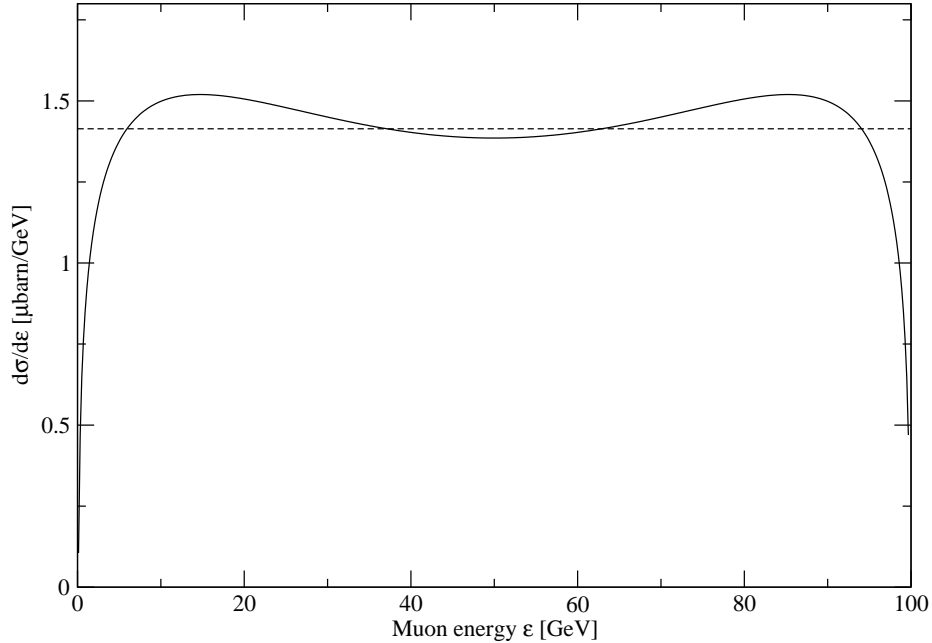


Figure 2: The differential Bethe-Heitler cross section $d\sigma/d\varepsilon$ for the generation of a muon of energy ε for an incident beamstrahlung photon with energy $\hbar\omega = 100$ GeV.

The water in the beam dump used to dissipate the energy of the incident photons will also cause the generation of muons, but this will require a detailed analysis because the attenuation of the photons will mostly be caused by the emitted e^+e^- pairs and only the remaining fraction can be used to generate muons. One might argue whether an extra converter is actually needed, and this needs to be investigated when optimizing the beam dump.

The momentum distribution of the muon pairs is given by the differential Bethe-Heitler cross section [8]

$$\frac{d\sigma}{d\varepsilon_+} = 4Z^2\alpha r_\mu^2 \frac{\varepsilon_+^2 + \varepsilon_-^2 + 2\varepsilon_+\varepsilon_-/3}{\hbar\omega} \left(\ln \left(\frac{2\varepsilon_-\varepsilon_+}{m_\mu c^2 \hbar\omega} \right) - \frac{1}{2} \right) \quad (5)$$

where ε_+ is the energy of one of the muons and we have $\varepsilon_+ + \varepsilon_- = \hbar\omega$. For a 100 GeV photon the cross-section is shown in Fig. 2 where we observe that it is rather constant over the entire kinematically accessible range. We therefore approximate the probability $P(\varepsilon, \hbar\omega)$ of finding a muon of energy ε from an incident photon with energy $\hbar\omega$ to be $P(\varepsilon, \hbar\omega) = 1/\hbar\omega$ just as was done in Refs. [5, 6]. This is equivalent of replacing the proper Bethe-Heitler cross section in Fig. 2 by the dashed line. Finally we have to

multiply the probability by a factor 2, because the Bethe-Heitler cross section gives the probability of finding *one* partner of the pair with energy ε , but we actually have a muon pair with *two* particles.

Muons are unstable particles with a lifetime of $2.2 \mu\text{s}$ in their rest frame but their high energy and the short distance between their creation at the converter at the entrance of the dump to the Cerenkov detector will make the decay rate negligible. Moreover, the muons will be attenuated very little on their passage through the rest of the water beam dump and shielding and will eventually enter the gas volume of the Cerenkov detector following the beam dump. Actually the muons already emit Cerenkov light in the dump, but that will be difficult to detect and distinguish from the Cerenkov light of e^+e^- pairs that are abundantly generated in the dump. But the muons are the only charged particles that can arrive at the external Cerenkov detector.

Once inside the gas volume of the Cerenkov detector the muons with speed β_μ will generate the following number of Cerenkov photons [9] per frequency

$$\frac{dN}{d\nu} = \frac{2\pi\alpha l}{c} \left(1 - \frac{1}{\beta_\mu^2 n^2}\right) \approx \frac{2\pi\alpha l}{c} \left(1 - \frac{1}{n^2} \left(1 + \frac{1}{\gamma_\mu^2}\right)\right) \quad (6)$$

where l is the length of the gas volume and $\gamma_\mu = 1/\sqrt{1 - \beta_\mu^2} = \varepsilon_\mu/m_\mu c^2$. We need to keep in mind that the emission of Cerenkov light has a threshold given by $\beta_\mu n < 1$ or $\gamma_\mu > \gamma_0 = n/\sqrt{n^2 - 1}$. For convenience we assume that we use the same gas as in the SLC beamstrahlung detector which was Ethylene at 1/3 bar resulting in a refractive index $n = 1 + 2 \times 10^{-4}$. The γ_0 describing the threshold for muons is therefore $\gamma_0 = 50$. This corresponds to a photon energy of 5.3 GeV and is a few times higher than the threshold required to suppress the synchrotron radiation from the chicane dipoles with a critical energy of 1.5 GeV.

In order to find the number of Cerenkov photons N as a function of incident beamstrahlung photon we have to convolute the muon creation probability with the Cerenkov photon generation probability and integrate over the intermediate muon energies. This results in [6]

$$N = nd\sigma \int_{\gamma_0}^{\hbar\omega} 2P(\varepsilon_\mu, \hbar\omega) \frac{dN}{d\nu} \Delta\nu d\varepsilon_\mu \approx nd\sigma \frac{4\pi\alpha l \Delta\nu}{c} \left(\frac{1}{\gamma_0} - \frac{1}{\gamma_B}\right)^2 \quad (7)$$

where we defined $\gamma_B = \hbar\omega/m_\mu c^2$ for notational convenience and assumed that the monitor detects Cerenkov photons within a frequency bandwidth $\Delta\nu$. For $\Delta\nu$ we assume a bandwidth of 5×10^{14} Hz which corresponds to the entire range of the visible spectrum ($\lambda = 0.3$ to $0.6 \mu\text{m}$). Inserting values from above and using a length $l = 1$ m for the gas volume we find

$$N = 0.18 \times \left(\frac{1}{50} - \frac{1}{\gamma_B}\right)^2 \quad \text{if } \gamma_B > \gamma_0 \quad (8)$$

which is shown in Fig. 3. We observe that we can expect on the order of $5 \times 10^{-5} = 1/20000$ Cerenkov photons per incident beamstrahlung photon of energy significantly above threshold of 5.3 GeV, say 50 GeV.

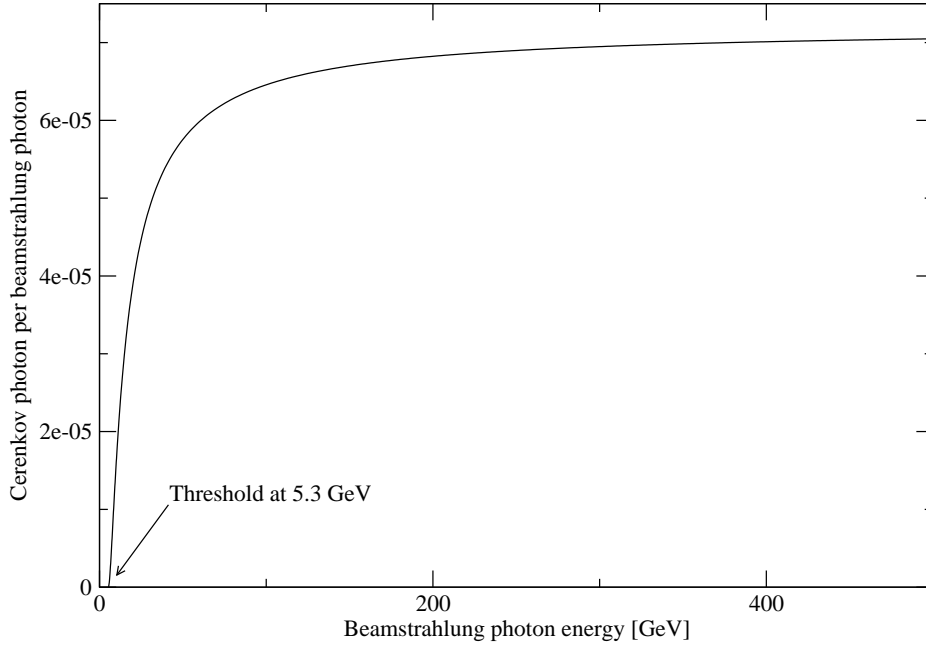


Figure 3: The production probability of Cerenkov photons within the visible range due to an incident beamstrahlung photon of energy $\hbar\omega$.

Considering that for standard CLIC parameters the number of beamstrahlung photons is on the same order of magnitude as the number of particles in the beam we can expect on the order of 4×10^9 photons of which most will exceed the threshold energy. Consequently we can expect on the order of 2×10^5 Cerenkov photons per bunch, which should be reliably detectable with a photo-multiplier. Detecting the photo current of the photo-multiplier with fast ADCs with GHz bandwidth, similar to what is done the BPM or RF signals in the test-stands at CTF3 will yield information about the luminosity even within a bunch train which only lasts on the order of 100 ns.

We expect only moderate background signals, because the muons generated by the shower cascade of the primary beam that have sufficiently high energy to trigger the Cerenkov detector will be strongly forward peaked. Low energy muons with energy below the Cerenkov threshold could more easily acquire sufficient transverse momentum to reach the Cerenkov detector, but they would not trigger the detector. This is, however, only a qualitative discussion and a more thorough GEANT simulation to optimize parameters is needed.

3 Coherent Pairs

The coherent pairs are partially separated in the vertical chicane. The partners with charge opposite to that of the primary beam are deflected onto a separate beam dump and the same-charge partners will follow the primary beam and due to their significantly lower energy will likely be lost in the collimators within the chicane [1]. The latter particles will be indistinguishable from the low-energy tail of the primary beam and cannot be used for diagnostic purposes other than a generic tail monitor, discussed below. In the remainder of this report we will tacitly assume that the primary beam consists of electrons and the opposite charge coherent-pair partners are positrons, to avoid awkward writing. The converse is, of course, applicable to the beam dump of the counter-propagating primary (positron) beam.

The positrons are directed to their own secondary beam dump and will be able serve as collision or luminosity monitor since the beam-beam interaction is the only source¹ that generates positrons on the secondary beam-dump. This feature will be especially useful during the initial search for collisions, when neither the beam sizes, the waist positions, nor the beam positions will be accurately known and any small signal that can be tuned on will be extremely valuable as a observable that can be tuned and heuristically improved until for example beam-beam deflection scans can be used to optimize parameters.

Since the total power in the coherent pairs is much lower (on the order of kW) than in the primary beam (approximately 14 MW), we can place more advanced detection devices before the secondary beam dump. Particularly, we suggest to use a device similar to a drift chamber, but more robust in order to deal with the kW load. The wires should be oriented horizontally to be able to determine the vertical distribution of the positrons on the beam dump. This provides information about the momenta of the detected particles, because all charged particles emanate from a well-defined source point, the IP. A caveat is in order, though: there will be muons generated in the collimation section in the beginning of the beam delivery system. There part of the primary beam is lost on the collimators and muons are created which will spread all over the place, but will cause an equal problem for the particle detector at the IP and the beamstrahlung detector above. We assume that spoilers for the muons will be installed between IP and collimators.

4 Beam Dump Thermometry

The beam dump of CLIC likely will be similar to the one for ILC and contain a vortex water whirl to absorb the beam power and distribute it over a large volume in order to avoid vaporizing the water. The deposited beam power of the primary beam and most of its secondary products exceeds 14 MW. This extreme power load will of course heat the water and the temperature need to be monitored for security reasons. Since

¹apart from beam losses and synchrotron radiation that produces e^+e^- pairs if hitting the beam pipe near the positron dump. This requires careful shielding, or possibly a threshold detector for high energy positrons.

the extracted beam in CLIC passes through a vertical chicane it is widened vertically and determining the vertical temperature distribution could yield some insight into the beam size on the target. For example a signal that would reliably indicate whether the beams are colliding and are therefore disrupted were helpful. We propose to use an interferometric setup that is based on monitoring the change in refractive index of water that depends on the temperature.

In Ref. [10] it was shown that the refractive index of water varies according to

$$n = 1.341 - 2.262 \times 10^{-5} T \text{ [K]} . \quad (9)$$

when keeping all other parameters such as pressure and wavelength at standard values given in Ref. [11]. Following Ref. [10] further and assume that the temperature distribution along the one arm of the interferometer follows a Gaussian temperature distribution

$$T(x) = T_0 e^{-x^2/2\sigma^2} \quad (10)$$

with peak temperature T_0 above the average water temperature and RMS width σ we find that the relative change in phase is given by

$$\Delta m = \frac{1}{\lambda} \int \Delta n(x) dx \approx 96.3 \sigma T_0 \quad (11)$$

where λ is the wavelength of light. We find that temperature changes of T_0 on the order of 1 degree and σ on the order of cm will result in changes of m on the order of unity. We could either use a Mach-Zehnder type interferometer as sketched on the left in Fig. 4 or of Michelson type as sketched on the right side in Fig. 4. The latter is probably the more attractive because it only needs a single entry window into the dump at the expense of requiring a mirror embedded in the beam dump. The Mach-Zehnder configuration will need two windows, but can operate without embedded mirrors. All windows should have an anti-reflex coating. We stress that only relative changes of the temperature could be measured.

The speed at which the temperature could be measured is probably from one bunch-train to the next, because thermal processes are definitely slower than the 100 ns that the bunch train lasts. The water dump will be designed in such a way as to transport away the heat generated by the beam between pulses.

We expect that it would be most useful to monitor the presence of a beam-tail to determine whether the beams are in collision. This is the situation indicated in Fig. 4, where one arm of the interferometer probes the temperature in a region that would be heated by a beam tail. Furthermore, one might envision to scan one arm of the interferometer vertically to determine the momentum distribution of the beam online. This could be done either by scanning a single laser beam, or installing several laser systems in parallel.

5 Tail Monitors

When the beams are in collision a very pronounced low-energy tail will be present in the primary beams in the post-collision line. These tails will deposit a significant amount

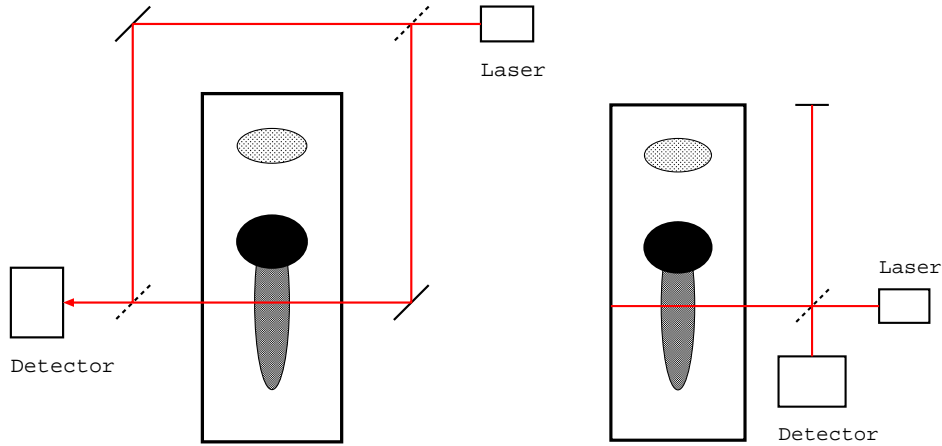


Figure 4: Mach-Zehnder interferometer (left) and a Michelson interferometer (right) to measure the vertical temperature distribution in the beam dump. The light-grey spot on the top represents the beamstrahlung impinging on the beam dump and the dark lower spot represents the main part of the primary beam if it is un-disrupted and the lighter region extending down shows the low-energy tail that develops when the beams are in collision. One arm of the interferometers passes the area where the tail develops and a temperature change causes a phase shift that is visible as a change of the interference pattern on the detector.

radiation into the collimators sandwiched between the individual dipoles of the chicane. An increased amount of radiation at these strategic locations will therefore be a signature of colliding beams and the amount is likely related to the luminosity. The large amount of radiation is, of course, a problem for diagnostic devices which tend to malfunction after a long period of exposure to high levels of radiation. A similar problem was present at DESY and was solved by the beam loss system of both the proton and the electron-ring of HERA [12]. There radiation detectors based on PIN diodes were successfully used to monitor beam losses, albeit at a lower rate than anticipated in CLIC.

A possible layout of such a detector, that was tested by the author several years back with 180 MeV protons and is based on reverse-biased PIN diodes (BPW-34) is shown in Fig. 5. The two diodes that should be wrapped in dark masking tape to avoid illumination by normal light operate in coincidence. They do not conduct when "dark" or unexposed to radiation, but will conduct when radiation hits them. The voltage drop over the 10k resistor is fed into a TLC-271 unipolar op-amp, that acts as a impedance converter to a $50\ \Omega$ line.

Such a detector could be embedded in the body of the collimators that are located between the dipole magnets that make up the chicane. Being inside the collimator and shielded by the adjacent dipoles will protect the diodes from radiation generated elsewhere but would expose them to the spray of particles caused by the primary particles directly impacting on the collimator. A detailed study with GEANT, MARS, EGS4 or

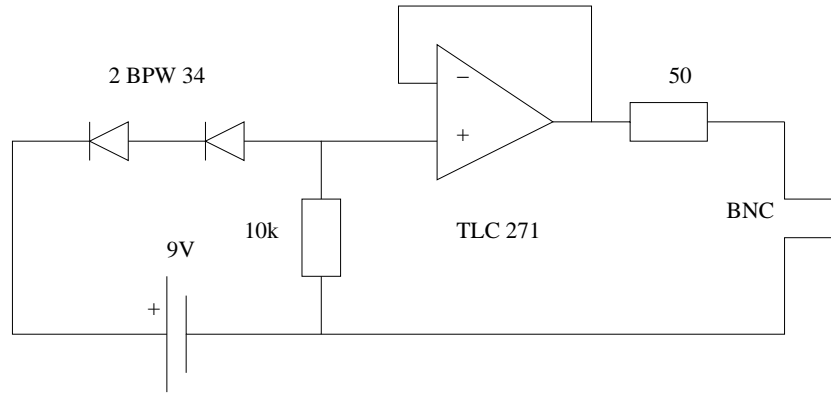


Figure 5: *Schematic of a simple radiation detector.*

other simulation programs is needed to determine how much signal the PIN radiation monitors are exposed to upon impact of a full energy electron or positron on the collimator. But this is relegated to the future. An important parameter to optimize is certainly the distance of the hole with the detector from the edge of the collimator. It should be as protected as possible, but, at the same time, as sensitive as possible to the radiation from direct beam impact on the collimator.

In the same spirit as the PIN detector, scintillation or other radiation detectors such as ionization chambers might be embedded deep in the collimators. By the same token as before the detector were protected by adjacent magnets, but sensitive by scatter products from direct impact.

6 Image Current Monitors

Another non-invasive means of detection can be accomplished by monitoring the image charges propagating in the beam chamber as is conventionally done by beam position monitors. The difference here is that the beam pipe is rather large and also has a large aspect ratio, because the vertical chicane in the post-collision line causes significant dispersion which will separate the primary beam particles according to their energy. If the beams are in collision a significant fraction of the particles will have rather low energies. This fraction of the beam is passing through the post-collision line at a vertical offset and, since the beam is ultra-relativistic the image charges will do likewise. Installing BPM like devices on the left and right side at several vertical positions of the vacuum pipe near the end of the post-collision line. A sketch is shown in Fig. 6 where the small capacitor-like devices on the left and right side indicate the button or strip-line monitors. We suggest to use the sum and difference of the left and the right monitors that reside on the same height as indicators of the amount of charge at the respective vertical position. First we want to point out that a strip-line detector is advantageous, because it can distinguish the primary beam on its way to the dump and charged particles moving backwards. The latter might be relevant to assess background in the detector at the IP.

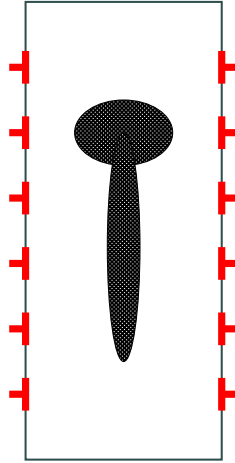


Figure 6: Detector for image charges traveling in the vacuum beam pipe.

In order to assess the sensitivity we use FEMLAB [13] to calculate the electric field perpendicular to the surface on the vertical boundary where the buttons in Fig. 6 are located due to point charges in the vacuum beam pipe and plot the resulting field in Fig. 7. We see that the small charge near the bottom with 10% of the charge near the top only marginally changes the electric field at the location of the monitor at the bottom near 0.8 m. Another run with a 1% charge near the bottom showed no discernible difference to the solid curve and we do not show it. For the strip line monitors we need to calculate the parallel magnetic field component along the vertical boundary, but the plots are equal, apart from the vertical scale, to those of the perpendicular electric field, because both calculations are based on solutions of Poisson's equation for the electric and magnetic potentials and therefore yield equal results, apart from the scale.

We conclude that the sensitivity of this method is poor, mostly due to the fact that the beam pipe is rather wide and the signal due to the main part of the beam spreads out along all monitors on the vertical beam pipe wall such that the contribution of a small part of the beam at another location is hardly visible.

7 Conclusion

For successful operation of CLIC fast signals that are related to the luminosity are necessary and need to be integrated in the detector or the post-collision beam line between IP and beam dump. The task is made complicated by the very high radiation levels will favor non-invasive systems. Furthermore, the parameter regime in which CLIC operates is different from any other accelerator and this makes it attractive to consider non-standard monitor systems. In this report we discuss five different systems that might be included into the post-collision line. Most attention was spent on the beamstrahlung monitor, which is an adaption of a system that was used successfully in the SLC. The coherent pair monitor was already designed into the CLIC post-collision

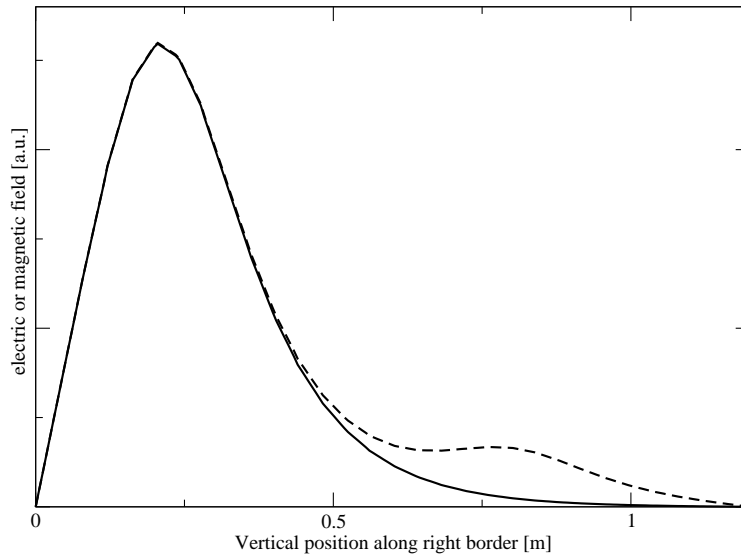


Figure 7: The perpendicular electric or parallel magnetic field along the right side of the vacuum beam pipe with width of 0.4 m and height 1.2 m. The solid line describes the field of a single point charge or current situated in the center of the pipe 0.2 m from the top and the dashed line that of the same charge or current with an added 10 % intensity 0.6 m further down at 0.8 m.

line. The next monitor type is based on measuring the change in refractive index of the water in the beam dump by interferometric means and the fourth is a tail monitor which is an adaption of a system that worked successfully in HERA. Finally, a system based on a modified BPM system that picks up the image currents from the beam tails in the highly elongated beam pipe proved less useful.

All monitors presented here are mere sketches of systems that need much more design work to establish their feasibility in CLIC, especially the coherent pair and tail monitor would benefit dramatically from simulations with particle tracking codes such as GEANT or BDSIM. This report should serve as a starting point for further discussions.

Acknowledgments

This work is supported by the Commission of the European Communities under the Sixth Framework Programme “Structuring the European Research Areas” under contract number RIDS-011899.

References

- [1] A. Ferrari, Conceptual design of a post-collision transport line for CLIC at 3 TeV, EUROTeV-Report-2007-001, CLIC note 704.
- [2] A. Ferrari, V. Ziemann, Conceptual Design of a vacuum window at the exit of the CLIC post-collision line, EuroTeV-Report-2008-009, CLIC Note 732.
- [3] P. Eliasson, M. Korostelev, D. Schulte, R. Tomas, F. Zimmermann, Luminosity tuning at the interaction point, Proceedings of EPAC 2006, p. 774.
- [4] R. C. Field, Beamstrahlung monitors at SLC, Nucl. Inst. and Methods A 265 (1988) 167.
- [5] E. Gero, The Theory and observation of classical beamstrahlung at the SLC, PhD thesis, University of Michigan, UMI-91-24010, 1991.
- [6] V. Ziemann, The response of the SLC beamstrahlung monitor, Single pass collider memo SLAC-CN-379, 1990.
- [7] V. Ziemann, Beamstrahlung simulation and diagnostics, SLAC-PUB-5595, Presented at the 7th ICFA Beam Dynamics Workshop, Los Angeles, CA, May 13-16, 1991.
- [8] L. Landau, E Lifschitz, *Relativistische Quantentheorie*, Akademie Verlag, Berlin, 1980
- [9] W.-M. Yao et al., Journal of Physics G 33 (2006) 1, available online at <http://pdg.lbl.gov>
- [10] V. Ziemann, Ideas for an Interferometric Thermometer, Nucl. Inst. and Methods A 564 (2006) 587
- [11] The International Association for the Properties of Water and Steam, “Release on the Refractive index of Ordinary Water Substance as a Function of Wavelength, Temperature, and Pressure”, Erlangen, Germany, September 1997, available at www.iapws.org/relguide/rindex.pdf
- [12] K. Wittenburg, The PIN-Diode Beam Loss Monitor System at HERA, DESY-HERA-2000-003 and Proceedings of the Beam Instrumentation Workshop 2000, AIP conference proceedings Vol. 546 (2000) 3.
- [13] <http://www.comsol.com>